

THE INFLUENCE OF AN EXISTING VERTICAL STRUCTURE ON THE INCEPTION OF WAVE BREAKING POINT

Dogan Kisacik¹ and Peter Troch²

Vertical breakwaters and sea walls are frequently used structures to protect ports from sea actions like waves and high water levels. Vertical structures expose slowly-acting pulsating loads or more intense but shorter lasting impulsive loads. Prediction methods for wave loads to calculate hydraulic responses of these structures generally use the incident significant wave height, often defined in the water depth at the seaward toe of the structure (h_s). Where, wave breaking has significant influence on design wave heights. In addition, due to the result of the reflection or/and turbulence left from preceding waves, the inception of wave breaking point is different than the point in the case without vertical structures. Therefore, the hydraulic performance of load tests on vertical structures should be known.

The reflection coefficients C_r , measured at the toe of the foreshore, are categorized based on the breaker shapes. According to the results, C_r values between, 0.55 – 0.80, and 0.45 – 0.70 are found for breaker types BWSAT (breaking with small air trap) and BWLAT (breaking with large trap) respectively.

The margin between non-breaking and breaking waves is considered as the inception point of breaking. This point is compared with the breaking point for the measurements without the scaled model to determine the influence of the scaled model on the inception point of the wave breaking. It is seen that the existence of the model postpones the inception of wave breaking for some waves which would normally break without the presence of the scaled model.

The main objective of the present research is to improve methods to predict wave behaviour and breaker heights for increasing safety of structures constructed in the surf zone. In this particular research, small scale model tests were carried out to fulfill the above goals.

Keywords: Vertical structures; wave breaking; wave reflection; wave shoaling

1. INTRODUCTION

Most of the structures placed in a wave field will reflect some proportion of the wave energy. The wave reflection depends on the wave length L , the water depth h and the wave height H at the toe of the breakwater as well as on a number of structural parameters like: steepness and roughness of the seaward slope, porosity of the structure, height and length of the berm. The reflection performance is also affected by the amount of wave overtopping.

For vertical structures, this reflected energy may cause problems within adjacent areas by increasing wave disturbance. The reflection from a vertical structure is described by the reflection coefficient (C_r). It is simply defined as the ratio of reflected and incident significant wave heights (H_{sr} , H_{si}).

$$C_r = \frac{H_{sr}}{H_{si}} \quad (1)$$

In literature, the reflection characteristics of vertical structures are generally related to the surf similarity number or the Iribarren number (ξ) (Battjes 1974).

$$\xi = \frac{\tan\alpha}{(H_0/L_0)^{0.5}} \quad (2)$$

where, H_0 and L_0 are the wave height and wave length in deep water.

However, the surf parameter given in Equation 2 does not consider the effect of h_s . Therefore, an upgraded surf similarity number β , given by Yoo (1986), is considered in the following.

$$\beta = \frac{2 \cdot \tan\alpha^2}{k^2 h_s H} = \frac{\tan\alpha^2}{\pi k h_s (H/L)} = \frac{\xi^2}{\pi k h_s} \quad (3)$$

In which, k is the local wave number. For the simplicity, L , H and k values are calculated at h_s measured at the toe of the foreshore.

Many coastal structures are constructed in relatively shallow water depths where the larger wave heights that constitute the primary input parameters in structure design are significantly influenced by depth-limited breaking. Prediction methods to calculate hydraulic or stability responses of these

¹ Country Institute of Marine Sciences and Technology, Dokuz Eylül University, Turkey, Haydar Aliyev Boulevard 100, 35430 Inciralti - Izmir, Tel:+90 (232) 2785565/108, Fax:+90 (232) 2785082, dogan.kisacik@deu.edu.tr

² Department of Civil Engineering, Ghent University, Technologiepark 904, Ghent, 9052, Belgium, TEL.: +32(0)9/264.54.89, FAX: +32(0)9/264.58.37, Peter.Troch@UGent.be

structures generally use the incident significant wave height (H_s) as primary input variable, often defined in the water depth at the seaward toe of the structure (h_s).

In deep water, the breaker height is governed by the wavelength whereas in shallow water it is determined by water depth. Therefore, the two common breaker indices for shallow (γ_s) and deep water (γ_d) can be expressed as follows.

$$\gamma_s = \frac{H_b}{h_b} \quad (4)$$

$$\gamma_d = \frac{H_b}{L_b} \quad (5)$$

where, H_b is the breaker height, h_b is the water depth at the breaking point and L_b is the breaking wavelength.

It is possible to combine both expressions in single formula that is valid for all depths (Southgate et al., 1995).

$$\frac{H_b}{L_b} = \gamma_d \tanh \left[\tanh \left(\frac{h_b}{L_b} \right) * \frac{\gamma_s}{\gamma_d} \right] \quad (6)$$

For shallow water, ($\tanh x \approx x$) Equation 6 simplifies to Equation 4. For deep water, ($\tanh x \approx 1$) Equation 6 simplifies to Equation 5.

McCowan (1894) is the first researcher who derived $H_b/h_b = 0.78$. His assumption is based on the fact that a solitary wave breaks as its crest angle approaches a limiting value. At the limiting value the fluid velocity at the crest surpasses the celerity of the profile. However, Goda (2010) mentions that a value of 0.8261 is more accurate which is proposed by Yamada et al. (1968). From the field observations, it is found to be between $\gamma_s = 0.78 - 0.86$.

For deep water conditions, Michell (1893) found the limiting steepness as $\gamma_d = 0.142$. However, Goda (2010) underlined the misunderstanding of the definition of L in γ_d which is the length of finite amplitude waves. If the small amplitude wavelength is employed instead of the finite amplitude wavelength, the new γ_d is expressed as $\gamma_d = 0.1684$.

The method of linking shallow and deep water breaking criteria was first suggested by Miche (1944) who adopted Michell's (1893) condition periodic waves over arbitrary water depth.

$$\frac{H_b}{L_b} = 0.142 \tanh \frac{2\pi h_b}{L_b} \quad (7)$$

In the last century, tremendous numbers of formulas have been proposed to describe the incipient condition of wave breaking. Detailed reviews of the existing researches have been made by Galvin (1972), Sawaragi (1973), Rattanapitikon et al. (2003), Camenen and Larson (2007), and Goda (2010).

Liu et al. (2011) categorized the breaking wave formulas into four groups based on their formation types.

They describe the first type as the form of Equation 4 which is known as the McCowan (1894) type.

$$\frac{H_b}{h_b} = \gamma(\theta, \lambda_0) \quad (8)$$

where $\lambda_0 = H_0/L_0$ is the deep water wave steepness with H_0 being the incident wave height.

The second type is known as the Miche (1944) type formula which is shown in Equation 9.

$$\frac{H_b}{L_b} = \alpha(s, \lambda_0) \tanh \left[\xi(s, \lambda_0) \frac{2\pi h_b}{L_b} \right] \quad (9)$$

The third type is known as the Goda (1975) type formula (Equation 10). It is a form of Equation 9 by considering L_0 instead of L_b . It is also assumed that $\tanh x$ can be approximated as $1 - \exp(-1.5x)$.

$$\frac{H_b}{L_0} = \alpha'(s, \lambda_0) \left\{ 1 - \exp \left[-1.5 \xi'(s, \lambda_0) \frac{2\pi h_b}{L_0} \right] \right\} \quad (10)$$

The fourth one is known as the Munk (1949) type formula (Equation 11). It is developed based on the relation between the shoaling coefficient that results from the conservation of the energy flux and the local value of the relative water depth.

$$\frac{H_b}{H_0} = \beta(s) \left(\frac{H_0}{L_0} \right)^m \quad (11)$$

The main aspects of hydraulic performance of load tests on a vertical structure are wave shoaling, wave reflection, wave breaking and overtopping. This paper gives a summary of methods to predict wave

shoaling and breaking in a wave flume with uniform bed slope and wave reflection from vertical structures with overhanging cantilevering surfaces. The measured results are compared with literature values. The discussions here are primarily based on 2-D hydraulic model tests of regular waves.

Within this paper, an overview of the small scale model test set up will be provided. This will be followed by the definition of non-breaking and breaking waves. Then, the margin between non-breaking and breaking waves is considered as the inception point of breaking. This point is compared with the breaking point for the measurements without the scaled model to determine the influence of the scaled model on the inception point of the wave breaking.

2. EXPERIMENTAL SET-UP

Waves are produced in a 2-D wave flume. A model is located 22.5 m away from the wave paddle on a uniform slope (1/20) with 0.5 m depth at the location of the structure. The model is 0.3 m high. The physical model is built from a transparent thermoplastic material [poly(methyl methacrylate) (PMMA)] and instrumented with 10 sets of pressure sensors, 9 sets of wave gauges and a high speed camera (HSC). Wave gauges are used to monitor the wave information along the flume and at the scaled model location. Figure 1 shows the test set-up with and without the structure (Kisacik et al., 2012).

The high speed camera is used to record the development of waves before breaking on the structure as a function of time. The camera provides information on the breaking mechanism of waves and shape of impact which helps determining the types of breaker. Pressure sensors are used to register wave impact pressures as a function of time. The total force on the scaled model is calculated by integrating the pressure results.

The methods for the calculation of wave impacts on the structure, discussed in this research, are based on the incident waves at the location of the structure i.e. wave conditions as they will appear if the model is not there. Therefore, the tests conducted with the scaled model are repeated without the model present under similar hydraulic conditions to have the undisturbed wave conditions. After the location of the model, a passive absorption is installed using gravel beaches. The gravel beach slope is 1/50. For the case of without structure, the reflection from the foreshore and the gravel beach is less than 7%.

Reflection analysis has been performed for the tests with the scaled model using wave records of the first 3 wave gauges (gauge 1, 2 and 3) which were located about 10 m in front of the scaled model (see Figure 1). The standard 3-gauge-procedure of Mansard & Funke, (1980) is used for the analysis of regular and irregular wave tests in the frequency domain. The partial standing wave field in front of the model has to be analyzed to determine: (i) the incident wave parameters as input parameters for the wave load of the structure and (ii) the wave reflection and thus the wave energy dissipation at the structure.

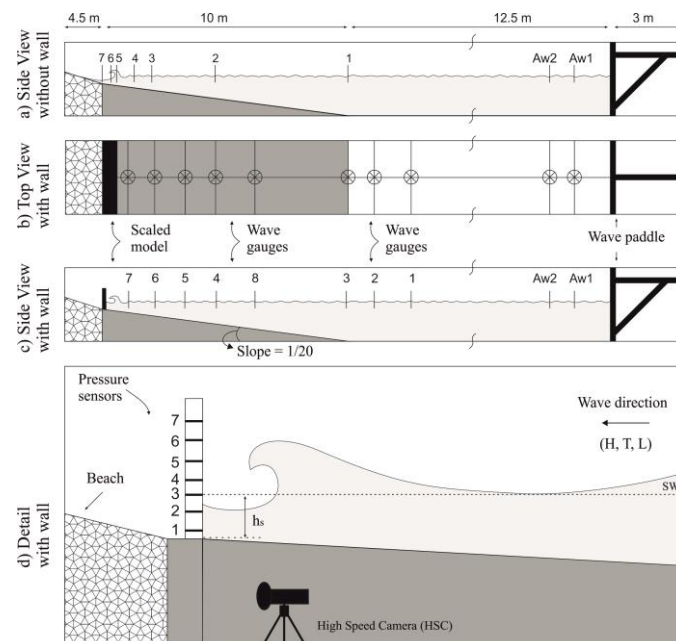


Figure 1. Small-scale model set up. a) is the side view without wall, b) is the top view with wall, c) is the side view with wall and d) is detailed view with wall

However, analyses for shoaling and wave breaking are conducted with the test results without scaled-model. As the wave propagates from offshore into shallow water, a number of different wave transformations will take place. When the water depth to wave length ratio becomes small, the sea bed influences the waves. Thus, the waves start to shoal, reducing the wave length, but increasing the wave height. Where water depths become even shallower, continuing shoaling of the waves, will lead some waves to approach the limiting value of steepness. Thereafter, any further increase will lead to wave breaking.

3. HYDRODYNAMIC CONDITIONS

Vertical structures which are standing against the waves reflect some of the incident waves while others break on the structure. Due to waves, vertical structures exposes dynamic and or quasi static forces and generally huge amount of overtopping can be seen. These forces depend on hydrodynamic parameters like wave height and wave period. The breaker types and the amount of reflection are also critical. In the following hydrodynamic processes of generated waves when they are approaching to the structure are discussed.

3.1 WAVE SHOALING

Most experimental studies on wave breaking have been on bed slopes shallower than 1:30, typically 1:50 or 1:100. On these slopes, wave shoaling is relatively mild, and wave breaking reasonably well understood. However, there is evidence that steep bed slopes transform waves differently and give more severe hydraulic and structural responses. In the following, wave heights on a bed slope of 1/20 measured along the channel are compared with Goda's (2010) theoretical approach.

In Goda's approach, $H_{1/3}$ and H_{max} values are the significant and maximum wave heights, respectively. The following expressions show how to calculate $H_{1/3}$ and H_{max} and they are valid for $H'_0/L_0 \leq 0.04$. If $H'_0/L_0 > 0.04$, then Figure 2 (Goda 2010) must be used.

$$\text{If } h/L_0 \geq 0.2 \rightarrow H_{1/3} = K_s H'_0 \quad (12)$$

$$\text{If } h/L_0 < 0.2 \rightarrow H_{1/3} = \min\{\beta_0 H'_0 + \beta_1 h, \beta_{max} H'_0, K_s H'_0\} \quad (13)$$

where,

$$\beta_0 = 0.028(H'_0/L_0)^{-0.38} \exp[20 \tan^{1.5} \theta]$$

$$\beta_1 = 0.52 \exp[4.2 \tan \theta]$$

$$\beta_{max} = \max\{0.92, 0.32(H'_0/L_0)^{-0.29} \times \exp[2.4 \tan \theta]\}$$

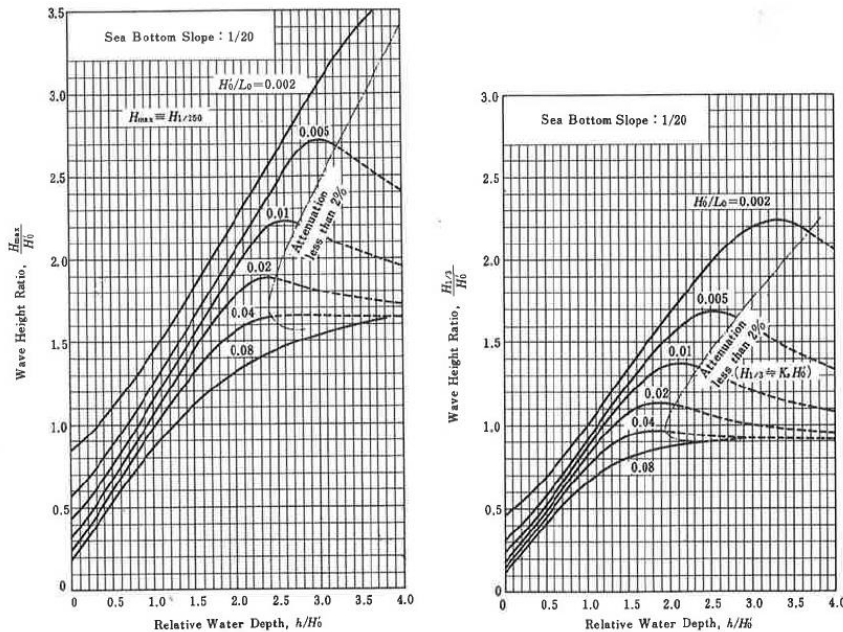


Figure2. Diagrams for the estimation of wave heights in the surf zone for sea bottom slope 1/20 (after Goda, 2000)

$$\text{If } h/L_0 \geq 0.2, H_{max} = H_{1/250} = 1.8K_s H'_0 \quad (14)$$

$$\text{If } h/L_0 < 0.2, H_{max} = \min\{(\beta_0^* H'_0 + \beta_1^* h), \beta_{max}^* H'_0, 1.8K_s H'_0\} \quad (15)$$

where,

$$\beta_0^* = 0.052(H'_0/L_0)^{-0.38} \exp[20 \tan^{1.5} \theta]$$

$$\beta_1^* = 0.63 \exp[3.8 \tan \theta]$$

$$\beta_{max}^* = \max\{1.65, 0.53(H'_0/L_0)^{-0.29} \times \exp[2.4 \tan \theta]\}$$

In the above equations, h is the water depth, H'_0 is the equivalent offshore wave height, L_0 is the offshore wave length related to the $T_{1/3}$, $\tan \theta$ is the foreshore slope and K_s denotes the shoaling coefficient. K_s can be calculated either from the below mathematical expressions or from graphs (Figure 3.26) in Goda (2010).

$$\text{If } h_{30} \leq h \quad \rightarrow K_s = K_{si}, \quad (16)$$

(K_{si} is the linear shoaling coefficient)

$$K_{si} = 1 / \sqrt{[(1 + (2kh)/\sinh(2kh)) \tanh(kh)]}$$

$$L = (g(T_{1/3})^2 / 2\pi) [\tanh(2\pi h/L)], \quad k = 2\pi/L$$

$$\text{If } h_{50} \leq h < h_{30} \quad K_s = (K_{si})_{30} \left(\frac{h_{30}}{h}\right)^{\frac{2}{7}} \quad (17)$$

$$\left(\frac{h_{30}}{L_0}\right)^2 = \frac{2\pi H'_0}{30 L_0} (K_{si})_{30}$$

$$(K_{si})_{30} = 1 / \sqrt{[(1 + (2kh)/\sinh(2kh)) \tanh(kh)]}$$

$$k = (k)_{30} = 2\pi / (L)_{30}, \quad (L)_{30} = (gT_{1/3}^2 / 2\pi) [\tanh(2\pi h_{30} / (L)_{30})]$$

$$\left(\frac{h_{50}}{L_0}\right)^2 = \frac{2\pi H'_0}{50 L_0} (K_s)_{50}$$

h_{30} and h_{50} are the water depth satisfying Equation 17 and Equation 18 respectively.

$$\text{If } h < h_{50} \quad K_s (\sqrt{K_s} - B) - C = 0 \quad (18)$$

$$B = \frac{2\sqrt{3}}{\sqrt{2\pi H'_0 / L_0}} \frac{h}{L_0}, \quad C = \frac{C_{50}}{\sqrt{2\pi H'_0 / L_0}} \left(\frac{L_0}{h}\right)^{\frac{3}{2}}$$

$$C_{50} = (K_s)_{50} \left(\frac{h_{50}}{L_0}\right)^{\frac{3}{2}} \left[\sqrt{2\pi H'_0 / L_0 (K_s)_{50}} - 2\sqrt{3} \frac{h_{50}}{L_0} \right]$$

Figure 3 shows the variation of the measured wave heights along the wave flume due to shoaling. Measurements are done at 8 different gauge locations ($h_s = 0.135 \text{ m}$). These are wave heights measured when the scaled model is not present in the flume. The gauge 7 is installed at the location of the scaled model. The lower and upper lines represent $H_{1/3}$ and H_{max} , are calculated according to Goda's theoretical approach.

Figure 3a to d show examples of wave shoaling selected in non-breaking, slightly breaking, breaking and broken waves. For each case, a single test is run and it shows the results of 14 uniformly developed waves. Along the horizontal bottom (out of the surf zone), all measured values are lying on the line of $H_{1/3}$. However in the surf zone (gauge 3, 4, 5, 6 and 7), scatter in the wave heights is increasing and measured values are closer to the H_{max} lines. The amount of scatter is more significant for the so called slightly breaking and breaking waves (Figure 3b and c). In these cases some values measured at gauges 5 and 6 are even higher than the H_{max} values. Figure 3d shows shoaling for the case of broken waves in which most of the waves break early and only turbulence reaches to gauge locations 5, 6 and 7. Therefore, measured wave heights in these locations are lower than the $H_{1/3}$ line.

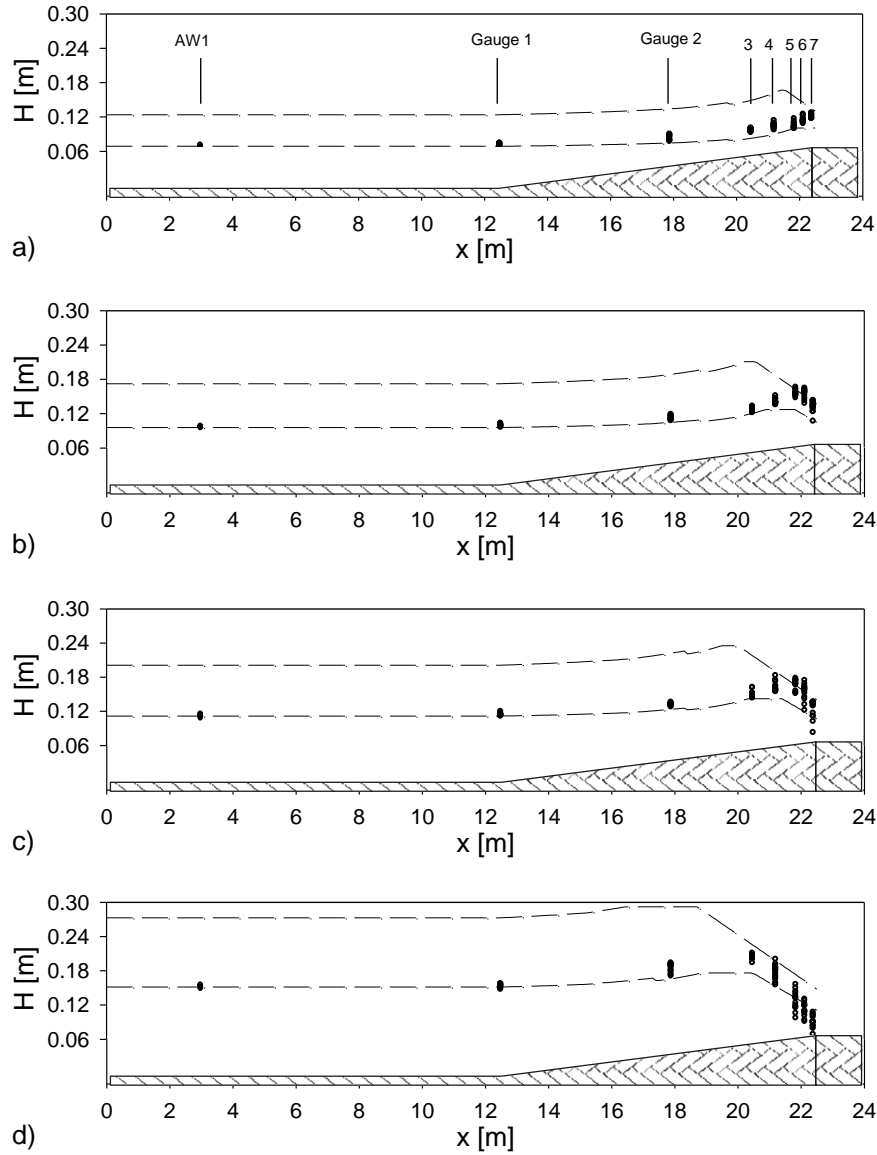


Figure 3. Measured wave heights at eight locations along the flume cross-section. Results are compared with calculated Goda values of $H_{1/3}$ and H_{max} . a) $H_{Target} = 0.07$ m, b) $H_{Target} = 0.095$ m, c) $H_{Target} = 0.11$ m and d) $H_{Target} = 0.145$ m.

3.2. WAVE REFLECTION

In Figure 4, the wave reflection due to the scaled model at the toe of the foreshore is plotted against the surf similarity number (β) for both regular and irregular waves. The scatter in regular wave results is mainly due to defining only one single Cr value for all 14 waves in one single test run. Therefore, a certain range of β is represented by a single Cr value. For irregular waves, H_{m0} and T_p values, measured at defined h_s , are considered for β calculations. H_{m0} is the significant wave height being estimated from the spectral information and T_p is the wave period corresponding to the frequency at the spectral peak. The irregular wave reflection analysis has been performed for a complete wave train of about 500 waves. Equation 19 and Equation 20 show the adopted line functions for regular and irregular waves.

Regular waves

$$C_r = -23.7\beta^2 + 10.3\beta - 0.2 \quad (19)$$

Irregular waves

$$C_r = -11\beta^2 + 5\beta + 0.2 \quad (20)$$

The regular wave reflection is increasing with increasing β . The maximum C_r is about 0.92 for the regular waves and about 0.80 for irregular waves. However, the minimum C_r is about 0.33 for regular waves and 0.56 for irregular waves. Normally, in a test run with uniformly distributed regular waves with small H values (non-breaking waves), most of the waves reflect from the scaled model with high C_r values. In the same manner, uniformly distributed regular waves with high H values break before reaching the model and C_r values will be low. However, in irregular wave terrain there are always some waves that break and some not. Therefore, the maximum C_r value is lower and minimum C_r value is higher for irregular waves compared to the C_r values for regular waves with equivalent wave heights.

Figure 5 shows the same data set shown in Figure 4. In this plot, C_r results are categorized based on breaker shapes as; slightly breaking waves (SBW), breaking with small air trap (BWSAT), breaking with large trap (BWLAT) and broken waves (BW). For vertical structures under non-breaking waves or SBW, the reflection is nearly total. Allsop (1999) summarized the wave reflection performance as:

$$C_r = 0.85 - 1.00 \tag{21}$$

In Figure 5 the range of C_r for SBW is close to the range recommended in Equation 21 and measured between $C_r = 0.80 - 0.92$. In addition, a few points are observed at $C_r < 0.80$. These points are probably errors occurring due to the measuring techniques which consider one C_r value for all 14 waves in one single test run.

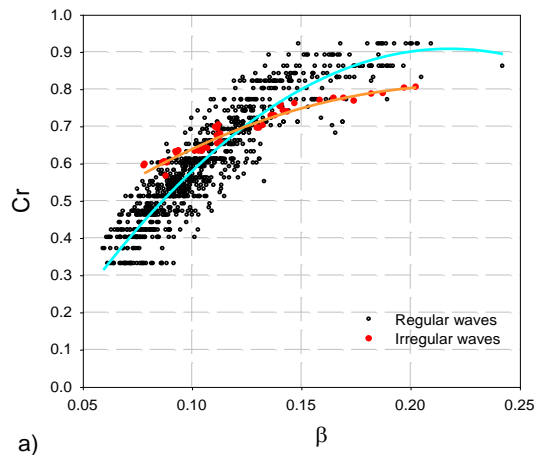


Figure 4. Variation of reflection coefficient, C_r , with the variation of surf similarity number, β

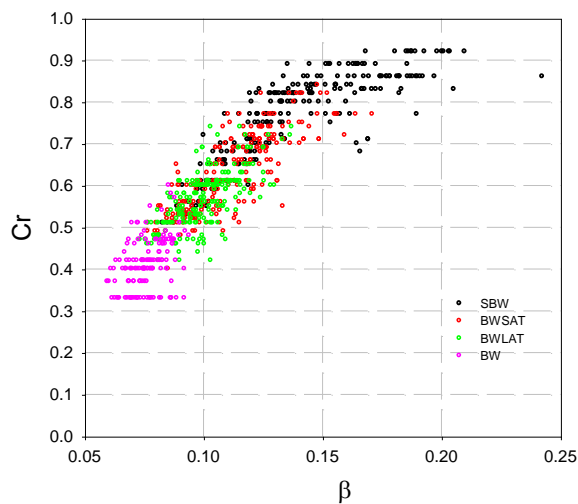


Figure 5. Variation of reflection coefficient, C_r , with the variation of surf similarity number, β . Different colors show the different breaking types. ($h_s = 0.135\text{ m}$)

Allsop (1999) suggested that the reflection coefficient for breaking waves might be assessed from:

$$C_r = 0.70 - 0.90 \text{ (for little breaking)} \quad (22)$$

$$C_r = 0.50 - 0.70 \text{ (for heavy breaking)}$$

The measurements in this particular research do not have a boundary as clear as mentioned by Allsop. The measured ranges of C_r are as follows:

$$C_r = 0.55 - 0.80 \text{ (BWSAT)} \quad (23)$$

$$C_r = 0.55 - 0.80 \text{ (BWLAT)}$$

On a simple vertical wall type structure, the degree of overtopping influences C_r values. As the crest level of the wall is reduced, more energy is transmitted rather than reflected, and C_r is reduced. However, overtopping is not allowed during this particular research, due to the spatial shape of the scaled model. Since differences in overtopping condition will be a reason for the differences between measurements and literature values.

For the BW, most of the wave energy dissipated due to the breaking, thus potentially reducing reflections. Since, the range of measured C_r for BW is between 0.33-0.50.

3.3. WAVE BREAKING

For engineering applications, Goda's (1970, 1975 and 2010) formula seems to have gained the best reputation. For regular waves, he considered $\alpha'(s, \lambda_0)$ as 0.17 and $\xi'(s, \lambda_0)$ as $1 + 11\theta^{4/3}$. Then Equation 10 simplifies to Equation 24.

$$\frac{H_b}{L_0} = A \left\{ 1 - \exp \left[-1.5 \frac{\pi h_b}{L_0} (1 + 11s^{4/3}) \right] \right\} \quad (23)$$

Figure 6 shows the comparison of measured breaking wave heights with the calculated breaking wave heights using the Goda (2010) method. Wave height values are measured from laboratory tests without scaled model. So, the results are not influenced by the existence of the model. The x-axis represents the horizontal distance along the flume from the paddle of the wave generator. The top bar of the x-axis shows the location of the gauges. The bottom figure displays the bed profile. Measurements are taken from 8 different locations of wave gauges (see Figure 3). At each gauge location, the highest measured wave height is considered as the measured value for the gauge. Wave gauge results are combined using solid lines, whereas calculated values are combined using dashed lines. For each water depth, the wave height increments are chosen as to have waves varying from non-breaking to broken at the location of the model. Therefore, only the highest

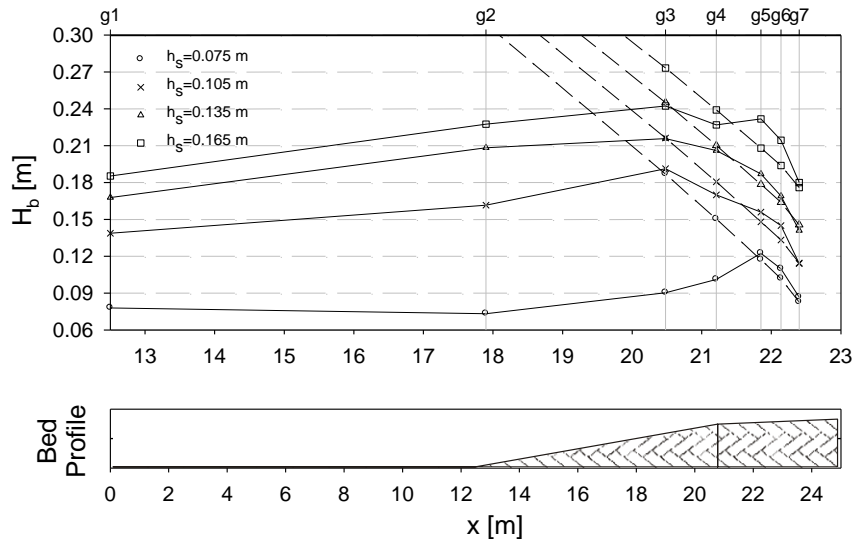


Figure 6. Comparison of measured breaking wave heights H_b (solid lines) with the calculated breaking wave height from Goda (2010) formula (dashed lines).

wave heights measured at gauges 5, 6 and 7 (located close to the model) are reaching the height of breaking wave heights. Consequently, measured wave heights at gauges 1 to 4 are lower than the calculated breaking wave heights. Even so, calculated values by the Goda method are underestimating the values at the location of gauge 7. Thus, the Goda method is calibrated by considering a new value $A = 0.21$, instead of 0.17. The difference between Goda and the measurements will be the difference in observation criteria that considered the highest wave height as the H_b .

4. THE INCEPTION POINT OF WAVE BERAKING

Figure 7 shows the inception of wave breaking points for four different values of h_s . The top figure displays the variation of the wave height (H_7) measured at the model location with the variation of the wave height (H_1) measured at the toe of the foreshore. As described before, tests are conducted under the same test matrix with and without installation of the model. H_7 and H_1 are the results of waves recorded under identical conditions, but without the model. Therefore, wave heights are not influenced by the model existence. As seen previously, wave heights are slowly increasing up to the breaking wave height which is considered the highest wave height at the location of the gauge. Then, already broken waves are approaching the gauge location. Due to the chaotic nature of the breaking, some high wave heights can also be recorded after the breaking point. Therefore, a polynomial line of regression analysis is adapted to the scatter data. The crest point of adopted line is considered as the breaking wave height. The second figure shows the variation of the maximum pressure at the vertical wall with the variation of H_1 . Pressure results are categorized as non-breaking and breaking waves. The appearance of breaking waves shows the inception point of wave breaking. Mainly, breaking wave results are high dynamic pressures whereas non-breaking wave results are low quasi-static pressures. The third figure is a detailed version of the second one which shows the scattering of non-breaking wave results in the breaking wave zone in detail. This scatter is caused by the appearance of the wall on the inception of wave breaking. The last figure shows the p_{max} values of the third wave results. The third wave is already well developed but less affected by disturbances originating from the two preceding waves. The transition from non-breaking waves to breaking waves is clear and the influence of the wall on the inception of wave breaking is zero or limited.

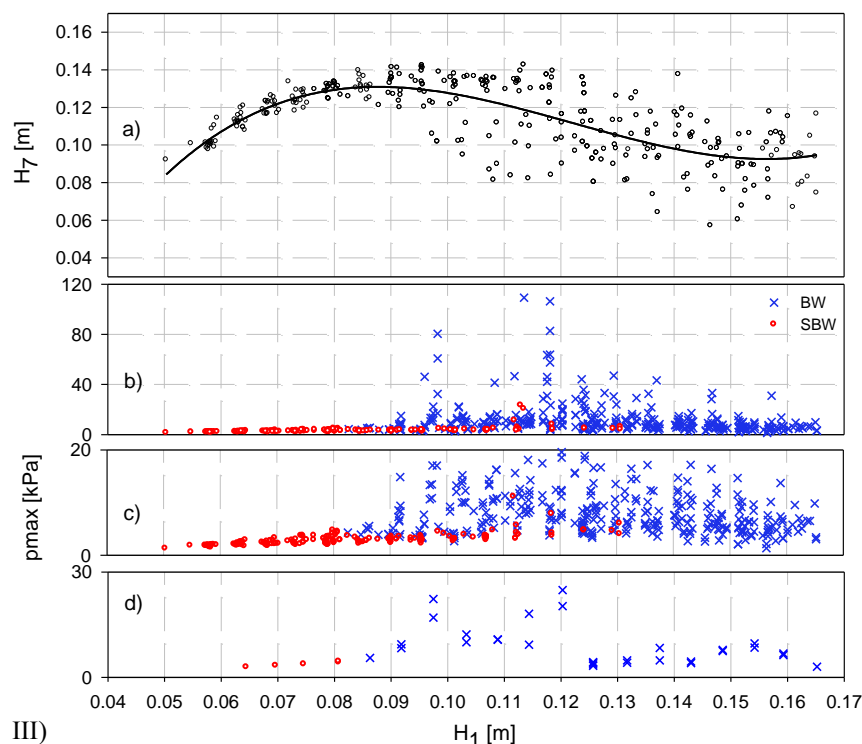


Figure 7. Inception of wave breaking points a) Variation of wave height (H_7) measured at the model location with the variation of wave height (H_1) measured at the toe of the foreshore. b) Variation of maximum pressure on the vertical part c) Variation of maximum pressure measured from the impact of 3th wave which is unaffected by the preceding waves ($h_s = 0.135$ m)

From Figure 7, it can be seen that both the transition points from non-breaking to breaking waves on the results of the third waves (d) and the inception points of breaking waves (a), the location of the highest H_g , are coinciding on the same H_1 values. These show that the third waves are less affected by the preceding waves and the criteria applied for distinguishing non-breaking and breaking waves work properly. However, the scatter of p_{max} values on (b) and (c) shows that the existence of the model postpones the inception of wave breaking for some waves which would normally break without the presence of the model. This postponing is the result of reflection or/and turbulence left from preceding waves. In addition, the influence of the wall on the inception point of breaking is increasing with rising water depth. This is in parallel with the increase of reflection amount in the higher water depths.

5. CONCLUSIONS

Wave shoaling, reflection, breaking and overtopping are the main hydraulic aspects considered for the performance of the scaled model test of a vertical structure with overhanging cantilevering surface. Tests are conducted in a 2-D wave flume with a uniform foreshore slope of 1/20. Wave gauges are used to monitor the wave information along the flume and at the scaled model location.

Wave shoaling has been analyzed for regular waves with test results without the pressure of the scaled-model. In this aspect, wave height variations along the flume are compared with calculated values of $H_{1/3}$ and H_{max} based on Goda's theoretical approach for shoaling. Along the horizontal bottom (out of the surf zone), all measured values are on the line of $H_{1/3}$. However in the surf zone, the wave heights are increasing due to shoaling and the measured values are closer to the H_{max} lines.

In addition, the wave reflection is analyzed for regular and irregular waves. The reflection coefficients C_r , measured at the toe of the foreshore, are categorized based on the breaker shapes as: slightly breaking waves (SBW), breaking with small air trap (BWSAT), breaking with large trap (BWLAT) and broken waves (BW). These results are compared with findings of Allsop (1999). According to the results, C_r values between 0.80 – 0.92, 0.55 – 0.80, 0.45 – 0.70 and 0.33 – 0.50 are found for SBW, BWSAT, BWLAT and BW respectively.

The breaking process has finally been analyzed for regular waves. Breaking wave heights, measured from laboratory tests without the scaled model, are compared with the calculated breaking wave heights using the Goda (2010) method. The Goda method is underestimating the values at the location of scaled model. Thus, the Goda method is calibrated by considering a new value $A = 0.21$, instead of 0.17.

Pressures on the scaled model are categorized as non-breaking and breaking waves. The margin between non-breaking and breaking waves is considered as the inception point of breaking. This point is compared with the breaking point for the measurements without the scaled model to determine the influence of the scaled model on the inception point of the wave breaking. It is seen that the existence of the model postpones the inception of wave breaking for some waves which would normally break without the presence of the scaled model. This postponing is the result of the reflection or/and turbulence left from preceding waves. In addition, the influence of the wall on the inception point of breaking is increasing with rising water depth.

REFERENCES

- Allsop, W., 1999, "Reflection coefficients", Probabilistic design tool for the vertical walls, volume IIa – Hydraulic aspects, pp 13
- Battjes, J. A., 1974, "A Computation of Set-Up, Longshore Currents, Run-Up and Overtopping Due to Wind-Generated Waves," Ph.D. diss., Delft University of Technology, The Netherlands
- Camenen B., Larson, M. (2007), Predictive Formulas for Breaker Depth Index and Breaker Type, -Journal of Coastal Research-2007-Vol-23-Issue-4-pp-1028-1041
- Galvin, C.J., Jr., (1968), Breaker Type Classification on Three Laboratory Beaches, Jour. Geophys. Res., 73(12), 3651,
- Goda, Y., 1970. A synthesis of breaker indices. Transactions of Japan Society of Civil Engineers 2, 39–49.
- Goda, Y., 1975. Irregular wave deformation in the surf zone. Coastal Engineering in Japan 18, 13–26.
- Goda, Y., 2010. "Reanalysis of regular and random breaking wave statistics". Coastal Engineering Journal 52 (1), 71–106.
- Kisacik, D.; Troch, P.; Van Bogaert, P., 2012, "Description of loading conditions due to violent wave impacts on a vertical structure with an overhanging horizontal cantilever slab", Coastal Engineering, Volume 60, Issue 1, February 2012, Pages 201-226

- Mansard, E. P. D., Funke, E. R., (1980), Measurement of incident and reflected spectra using a least squares method, -National Conference Publication-Institution of Engineers-n-80/1-pp-95-96
- McCowan, J. [1894] “*On the highest waves in water,*” Phil. Mag. Ser. 5, 36: 351-358.
- Miche, R. (1944). Mouvements ondulatoires de la mer en profondeur constante ou décroissante, Annales des Ponts et Chaussées, Vol. 114, 25–78, 131–164, 270–292, 369–406 (in French).
- Michell, J.H., 1893. On the highest waves in water. Philosophical Magazine 36, 430–435 Ser. 5.
- Munk, W.H., 1949. “*The solitary wave theory and its applications to surf problems*”. Annals of the New York Academy of Sciences 51, 376–462.
- Rattanapitikon, W., T. Vivattanasirisak and T. Shibayama, (2003) A Proposal of New Breaker Height Formula, Coastal-Engineering-Journal-2003-Volume-45-no-1-pp-29-48
- Sawaragi, T. and K.Iwata (1973), Some Considerations on Hydraulic Characteristic of perforated breakwater Quay, Proc. J. S. C. E. No 220
- Southgate, H.N., 1995. “*Prediction of wave breaking processes at the coastline*”. In: Rahman, M., Editor, , 1995. Advances in Fluid Mechanics vol. 6, Computational Mechanics Publications, Southampton, UK.
- Yamada, H., Kimura, G. and Okabe, J. [1968] “*Precise determination of the solitary waves of extreme height on water of a uniform depth,*” Rep. Res. Inst. Applied Mech., Kyushu Univ. XVI (52): 15-32.
- Yoo, D. (1986), Mathematical modelling of wave-current interacted flow in shallow waters, University of Manchester,
- Yu Liu, Xiaojing Niu, Xiping Yu, 2011 “*A new predictive formula for inception of regular wave breaking*”, Coastal Engineering, Volume 58, Issue 9, September 2011, Pages 877-889